

**Generalized analytical solutions for secure transmission of signals
using a simple communication scheme with numerical and
experimental confirmation**

G. Sivaganesh

*Department of Physics, Alagappa Chettiar College of Engineering & Technology,
Karaikudi, Tamilnadu-630 004, India*

A. Arulgnanam*

*Department of Physics, St. John's College,
Palayamkottai, Tamilnadu-627 002, India*

A. N. Seethalakshmi

*Department of Physics, The M.D.T Hindu College,
Tirunelveli, Tamilnadu - 627 010, India*

Abstract

A novel explicit analytical solution is reported for the transmission and recovery of information signals using a simple communication scheme. Analytical solutions are obtained for the normalized state equations of coupled second-order chaotic transmitter and receiver systems embedding the information signal. The analytical solution of the difference system obtained from the state equations of the transmitter and receiver systems has been identified as a measure of the recovered information signal which is transmitted securely by chaotic masking. The analytical solutions are used to reveal the nature of synchronization and the enhancement of the amplitude of recovered information signal. The difference signal of the coupled state variables indicating the recovered information signal obtained through numerical simulations is presented to validate the analytical results. The electronic circuit experimental results are presented to confirm the analytical and numerical results of the communication scheme discussed.

PACS numbers: 05.45.Xt, 05.45.-a

Keywords: chaos; synchronization; signal transmission

*Electronic address: gospelin@gmail.com

I. INTRODUCTION

The concept of secure communication using chaotic carrier signals has its origin in the phenomenon of chaos synchronization. Following the *master-slave* concept of chaos synchronization introduced by Pecora and Carroll [1], a variety of complex dynamical systems have been studied for synchronization [2–6]. The method proposed by Pecora *et al.* involves the synchronization of a *slave* sub-system with a *drive* subsystem. The synchronization phenomena observed in electronic circuit systems has been used for the secure transmission of information signals through chaotic masking i.e. *spread spectrum communications* [3, 5, 7–10] and for signal transmission through image encryption [11–13]. Further, several electronic circuit systems with chaotic and hyperchaotic behavior have been designed and analyzed for the implementation of secure transmission of signals [14–20]. Synchronization is also observed in coupled chaotic systems by unidirectional (one-way) coupling of the master and slave systems using a common chaotic signal without constructing any stable subsystems. This method has been successfully implemented to achieve synchronization and for signal transmission by chaotic masking of the information signal [5, 8]. The identification of chaotic dynamics in a second-order, non-autonomous chaotic circuit by *Murali et al.* [21] has opened the gateway for designing several simple circuit systems with high complex dynamics [22–24]. The piecewise-linear nature of the nonlinear elements present in these simple systems makes their dynamics to be mathematically tractable. The dynamical process of chaos synchronization observed in unidirectionally and mutually coupled simple chaotic systems have been greatly studied through explicit analytical solutions, numerical simulations and confirmed experimentally [25–28]. A mathematical analysis based on the time series of the state variables has been presented for the synchronization and signal transmission using chaos in the quadratic and *Ueda* systems [29]. However, an explicit analytical solution for the normalized state equations of the coupled transmitter and receiver systems explaining the transmission and recovery of information signals using simple chaotic systems is yet to be studied. The mathematical tractable nature of the systems may provide new insights on the synchronization dynamics of the systems upon signal transmission.

This paper is aimed at presenting a novel generalized explicit analytical solution for the

transmission and recovery of information signals using the simple communication scheme proposed by *Murali et al.* [8] using the chaotic carrier signals obtained from a class of simple second-order chaotic systems. The forced series *LCR* circuit system with two types of piecewise-linear elements namely, the *Chua's diode* and the *simplified nonlinear element (SNE)*, are studied for the transmission of information. The nature of the synchronization phenomena observed in the coupled systems upon the recovery of information signal is studied analytically. The analytical results thus obtained are validated through numerical and experimental results. This paper is divided as follows. In Sec. II we introduce a simple communication scheme and present the experimental results for the transmission of a signal by chaotic masking observed in coupled simple chaotic systems. The analytical and numerical results for signal transmission is presented in Sec. III and Sec. IV, respectively.

II. EXPERIMENTAL RESULTS

In this section, we present the experimental results on the design of a unidirectionally coupled transmitter and receiver to illustrate the retrieval of the information signal. The applicability of this method of chaos synchronization and signal masking approach to coupled non-autonomous series *LCR* circuit systems under the *drive-response* configuration is discussed. The physical implementation of the circuitry for chaos communication in a forced series *LCR* circuit is as shown in Fig. 1. The circuits on the left and the right side indicate the transmitter and receiver systems, respectively. The circuit equations governing the transmitter and receiver system with the information signal as shown in Fig. 1 can be written as

Drive - Transmitter:

$$C \frac{dv}{dt} = i_L - g(v), \quad (1a)$$

$$L \frac{di_L}{dt} = -Ri_L - R_s i_L - v + F_1 \sin(\Omega_1 t), \quad (1b)$$

Response - Receiver:

$$C \frac{dv'}{dt} = i'_L - g(v') + \epsilon(r(t) - v'), \quad (2a)$$

$$L \frac{di'_L}{dt} = -Ri'_L - R_s i'_L - v' + F_2 \sin(\Omega_2 t), \quad (2b)$$

where $g(v)$ and $g(v')$ representing the piecewise linear element given by

$$g(v) = G_b v + 0.5(G_b - G_a)[|v + B_p| - |v - B_p|], \quad (3a)$$

$$g(v') = G_b v' + 0.5(G_b - G_a)[|v' + B_p| - |v' - B_p|], \quad (3b)$$

The terms $\epsilon = \frac{R}{R_c}$ and $r(t) = v(t) + s(t)$ where, ϵ and $s(t)$ represent the coupling strength and the transmitted signal, respectively. The drive system operating at the double-band chaotic attractor state is used as the carrier wave to mask the information signal. The typical experimental information signal $s(t)$ is shown in Fig. 2a(i) and the experimentally observed double-band chaotic waveform, $v(t)$ observed across the capacitor C is shown in Fig. 2b(i). The chaotic signal $v(t)$ has been used as the carrier wave of this unidirectional scheme. In the absence of the signal $s(t)$, a synchronized chaotic behavior is observed in the coupled system between $v(t)$ and $v'(t)$ [27], for $\epsilon = 1105.5$, $C = 10.31$ nF, $L = 51.3$ mH, $R = 2211$ Ω , $F_{1,2} = 1.7$ V, $\nu_{1,2} = 5500$ Hz, $G_a = -0.56$ mS, $G_b = 2.5$ mS and $B_p = \pm 3.8$ V. When the power of the information signal $s(t)$ is comparably lower than the chaotic carrier signal $v(t)$ then $s(t)$ can be recovered as [30]

$$s(t) = r(t) - v'(t) = v(t) + s(t) - v'(t) \approx s'(t), \quad (4)$$

where $s'(t)$ represents the information signal recovered at the receiver system. Experimental observation of Fig. 2 gives rise to the information signal $s'(t)$ as recovered at the response system by adopting Eq. 4.

Figure 2a(i)-d(i) represents the experimentally observed time series of the sine wave indicating the information signal $s(t)$, the chaotic carrier wave $v(t)$ across the capacitor of the drive system, the amplitude modulated chaotic transmitted signal, $r(t) = v(t) + s(t)$ and the recovered information signal $s'(t)$, respectively. The amplitude modulated wave shown in Fig. 2b(i) indicates that the information signal has been completely masked by the carrier wave and retains its chaotic nature. Figures 2a(ii)-d(ii) represent the corresponding power spectrum of the information signal $s(t)$, chaotic carrier signal $v(t)$, the amplitude modulated transmitted signal $r(t)$ and the recovered information signal $s'(t)$, respectively. As the power level of the information signal $s(t)$ is significantly lower than that of the chaotic carrier signal $v(t)$, the frequency component of $s(t)$ is not detectable in Fig. 2c(ii) due to the broadband nature of the modulated transmitted signal. The identical nature of the wave form and power spectra of the information signal and the recovered signal shown in Fig.

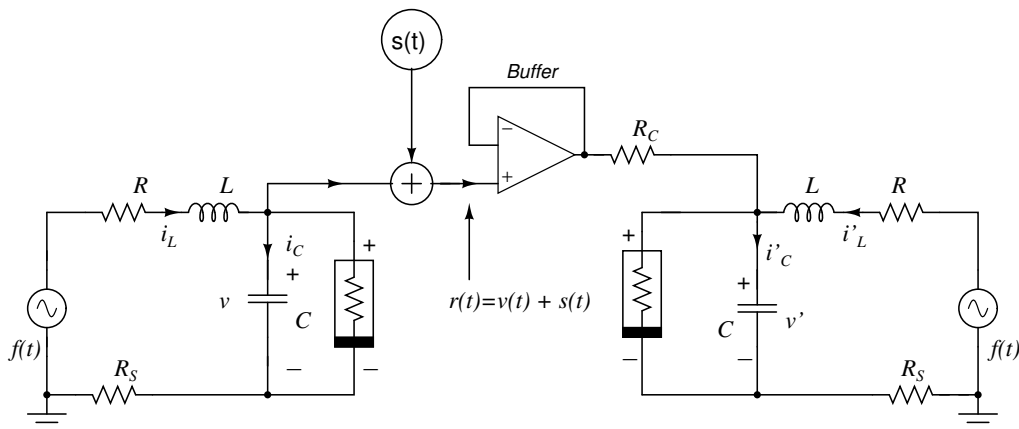


FIG. 1: Circuit realization of two forced series LCR circuits with unidirectional coupling for signal transmission.

2a(i), 2a(ii) and Fig. 2d(i), 2d(ii) indicates the successful retrieval of the information signal at the receiver. This communication scheme has been further tested with another type of information bearing signal, the square wave, as shown in Fig. 3. Figure 3a(i)-d(i) represents the experimentally observed time waveform of the information bearing signal $s(t)$ (a square waveform), the chaotic carrier waveform $v(t)$ of the drive system, the actual transmitted signal, $r(t) = v(t) + s(t)$ and the recovered signal $s'(t)$, respectively. Figures 3a(ii)-d(ii) represent the corresponding power spectrum of the information signal $s(t)$, chaotic signal $v(t)$, the actual transmitted signal $r(t)$ and the recovered signal $s'(t)$, respectively.

III. EXPLICIT ANALYTICAL SOLUTIONS

In this section, we present the explicit analytical solutions for the recovery of the information signal transmitted using a chaotic carrier signal. The analytical solutions are presented for the case of the information signal being a sine wave signal of the form $s(t) = f \sin(\omega t)$. The amplitude of the information signal is so chosen that it is lesser than that of the chaotic carrier wave. After proper rescaling, the normalized state equations of the transmitter and the receiver systems given in Eqs. 1 and 2 can be written as

Drive - Transmitter:

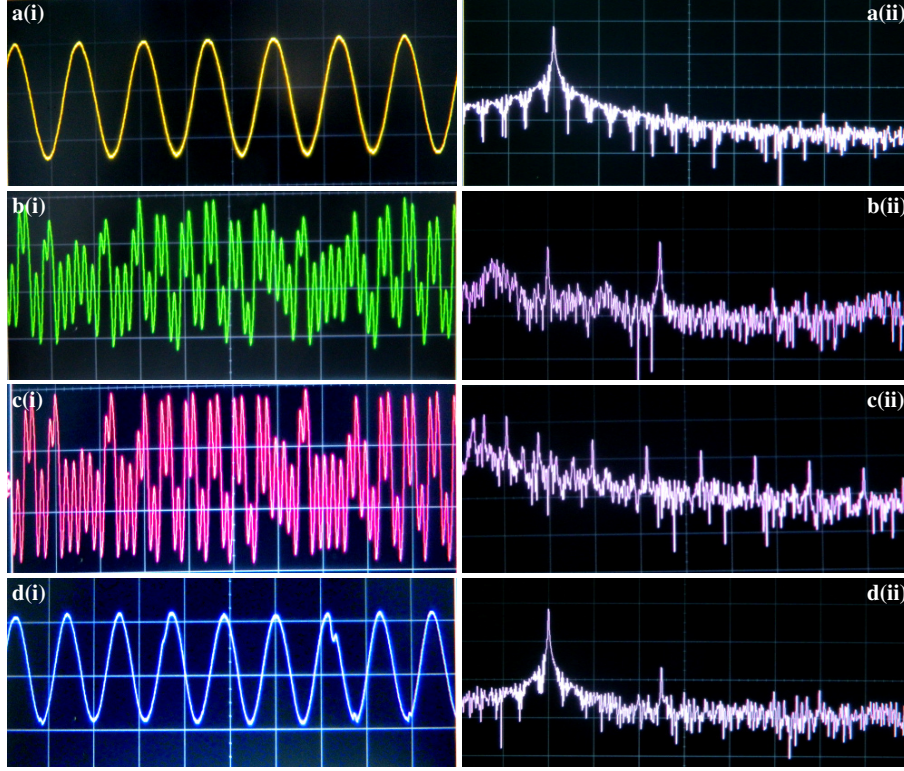


FIG. 2: Experimental implementation of the communication scheme observed using the unidirectionally coupled forced series LCR circuits indicating the (i) time series and the corresponding (ii) power spectrum of the signals; (a) sine wave information signal ($s(t) = F \sin \omega t$, $F = 0.5$ V, $\nu = 6280$ Hz); (b) chaotic carrier signal $v(t)$; (c) the amplitude modulated chaotic transmitted signal $r(t) = v(t) + s(t)$ and (d) the recovered information signal $s'(t)$ at the receiver.

$$\dot{x} = y - g(x), \quad (5a)$$

$$\dot{y} = -\sigma y - \beta x + f_1 \sin(\omega_1 t), \quad (5b)$$

Response - Receiver:

$$\dot{x}' = y' - g(x') + \epsilon(x + f \sin(\omega t) - x'), \quad (6a)$$

$$\dot{y}' = -\sigma y' - \beta x' + f_2 \sin(\omega_2 t), \quad (6b)$$

where $\beta = (C/LG^2)$, $\nu = GR_s$, $a = G_a/G$, $b = G_b/G$, $f_{1,2} = (F_{1,2}\beta/B_p)$, $\omega_{1,2} = (\Omega_{1,2}C/G)$ and $G = 1/R$. The term $f \sin(\omega t)$ represents the information signal and $g(x)$, $g(x')$ repre-

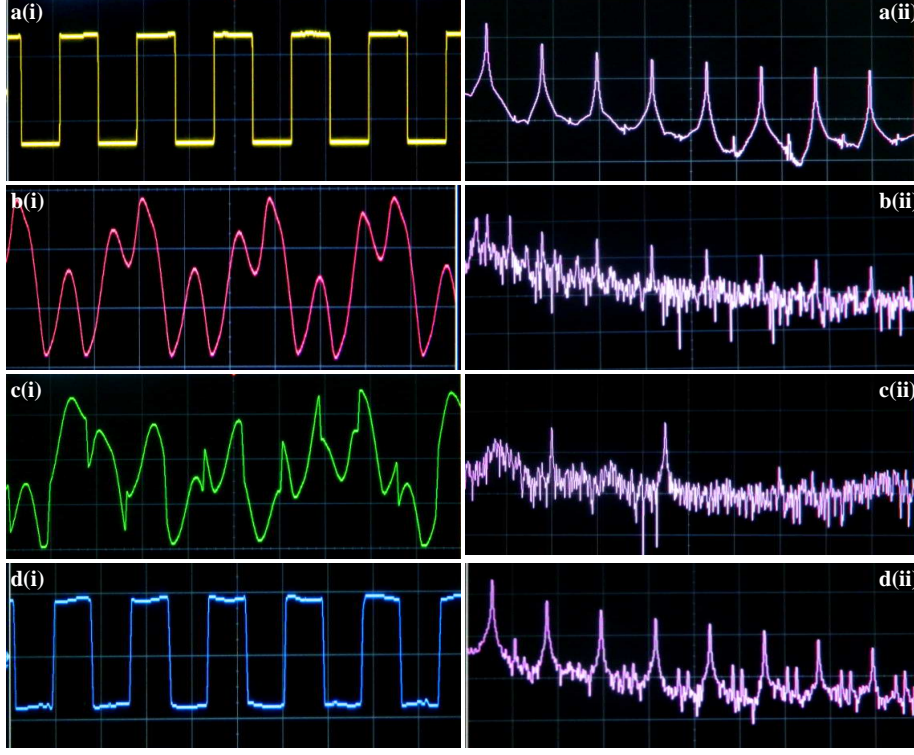


FIG. 3: Experimental implementation of the communication scheme observed using the unidirectionally coupled forced series *LCR* circuits indicating the (i) time series and the corresponding (ii) power spectrum of the signals; (a) square wave information signal ($s(t) = F \sin \omega t$, $F = 0.5$ V, $\nu = 6500$ Hz); (b) chaotic carrier signal $v(t)$; (c) the amplitude modulated chaotic transmitted signal $r(t) = v(t) + s(t)$ and (d) the recovered information signal $s'(t)$ at the receiver.

sents the nonlinear element given as

$$g(x) = \begin{cases} bx + (a - b) & \text{if } x \geq 1 \\ ax & \text{if } |x| \leq 1 \\ bx - (a - b) & \text{if } x \leq -1 \end{cases} \quad (7)$$

and

$$g(x') = \begin{cases} bx' + (a - b) & \text{if } x' \geq 1 \\ ax' & \text{if } |x'| \leq 1 \\ bx' - (a - b) & \text{if } x' \leq -1 \end{cases} \quad (8)$$

When ($\epsilon = 0$), the transmitter and the receiver systems are independent and the solutions are summarized as follows:

In the D_0 region, for complex roots, $y(t)$ and $x(t)$ are

$$y(t) = e^{ut}(C_1 \cos vt + C_2 \sin vt) + E_1 + E_2 \sin \omega_1 t + E_3 \cos \omega_1 t, \quad (9a)$$

$$x(t) = \frac{1}{\beta}(-\sigma y - \dot{y} + f_1 \sin \omega_1 t), \quad (9b)$$

and for real roots

$$y(t) = C_1 e^{m_1 t} + C_2 e^{m_2 t} + E_1 + E_2 \sin \omega_1 t + E_3 \cos \omega_1 t, \quad (10a)$$

$$x(t) = \frac{1}{\beta}(\dot{y}). \quad (10b)$$

In the $D_{\pm 1}$ region, for complex roots

$$y(t) = e^{ut}(C_3 \cos vt + C_4 \sin vt) + E_3 \sin(\omega_1 t) + E_4 \cos(\omega_1 t) \pm \Delta, \quad (11a)$$

$$x(t) = \frac{1}{\beta}(\dot{y}). \quad (11b)$$

and for real roots

$$y(t) = C_3 e^{m_3 t} + C_4 e^{m_4 t} + E_3 \sin \omega_1 t + E_4 \cos \omega_1 t \pm \Delta, \quad (12a)$$

$$x(t) = \frac{1}{\beta}(\dot{y}), \quad (12b)$$

The above solution is applicable for the receiver system operating with different initial conditions. For $\epsilon > 0$, the state equations of the transmitter and receiver systems given in Eqs. 5 and 6 gives rise to non-identical chaotic attractors owing to the presence of the information signal and the analytical solutions for retrieving the information signal can be deduced through suitable transformation of Eqs. 5 and 6. The transformation is the formulation of a difference system in each of the coupled, identical piecewise-linear regions of the transmitter and receiver systems and hence, the 4-dimensional coupled system has

been reduced to a 2-dimensional system. From Eqs. 5 and 6, the difference system can be written as

$$\dot{x}^* = y^* - (g(x) - g(x')) - \epsilon(x^* + f \sin(\omega t)), \quad (13a)$$

$$\dot{y}^* = -\sigma y^* - \beta x^* + f_1 \sin(\omega_1 t) - f_2 \sin(\omega_2 t). \quad (13b)$$

where $x^* = (x - x')$, $y^* = (y - y')$ and $g(x) - g(x') = g(x^*)$ take the values ax^* or bx^* depending on the region of operation. From the relations $r(t) = s(t) + x(t)$ and $x^*(t) = x(t) - x'(t)$, we get

$$s(t) = r(t) - x(t) = r(t) - x^*(t) - x'(t) \approx -x^*(t), \quad (14)$$

Hence, when the amplitude modulated signal $r(t)$ is nearly equal to the chaotic signal of the receiver system $x'(t)$, *i.e.* $r(t) \approx x'(t)$, the state variable $x^*(t)$ indicates a measure of the information signal retrieved at the receiver, given as

$$s'(t) = -x^*(t), \quad (15)$$

The above idea of the recovered signal $s'(t)$ can be confirmed by obtaining analytical solutions for the condition $\epsilon > 0$. Now, we find the solution of the state variables $x^*(t), y^*(t)$ in the regions D_0^* and $D_{\pm 1}^*$ of the difference system. Analytical solutions of this kind has been studied recently for synchronization in a number of systems [25–28]. Hence, we summarize the solution for the state equations of the difference system as follows.

A. D_0^* region

For real and distinct roots, the state variables are given as

$$\begin{aligned} y^*(t) = & C_1 e^{m_1 t} + C_2 e^{m_2 t} + E_1 \sin(\omega_1 t) + E_2 \cos(\omega_1 t) + E_3 \sin(\omega_2 t) \\ & + E_4 \cos(\omega_2 t) + E_5 \sin(\omega t) + E_6 \cos(\omega t) \end{aligned} \quad (16)$$

$$x^*(t) = \left(\frac{1}{\beta}\right)(\dot{y}^* - \sigma y^* + f_1 \sin(\omega_1 t) - f_2 \sin(\omega_2 t)) \quad (17)$$

The constants are

$$E_1 = \frac{f_1\omega_1^2(A - a - \epsilon) + f_1B(a + \epsilon)}{A^2\omega_1^2 + (B - \omega_1^2)^2} \quad (18a)$$

$$E_2 = \frac{f_1\omega_1((B - \omega_1^2) - A(a + \epsilon))}{A^2\omega_1^2 + (B - \omega_1^2)^2} \quad (18b)$$

$$E_3 = -\frac{f_2\omega_2^2(A - a - \epsilon) + f_2B(a + \epsilon)}{A^2\omega_2^2 + (B - \omega_2^2)^2} \quad (18c)$$

$$E_4 = -\frac{f_2\omega_2((B - \omega_2^2) - A(a + \epsilon))}{A^2\omega_2^2 + (B - \omega_2^2)^2} \quad (18d)$$

$$E_5 = \frac{\beta\epsilon f(B - \omega_2^2)}{A^2\omega_2^2 + (B - \omega_2^2)^2} \quad (18e)$$

$$E_6 = -\frac{A\omega\beta\epsilon f}{A^2\omega_2^2 + (B - \omega_2^2)^2} \quad (18f)$$

$$\begin{aligned} C_1 = & \frac{e^{-m_1 t_0}}{m_1 - m_2} \{(-\sigma y_0^* - \beta x_0^* - m_2 y_0^*) - (\omega_1 E_1 - m_2 E_2) \cos \omega_1 t_0 \\ & + (f_1 + \omega_1 E_2 + m_2 E_1) \sin \omega_1 t_0 - (\omega_2 E_3 - m_2 E_4) \cos \omega_2 t_0 \\ & + (\omega_2 E_4 + m_2 E_3 - f_2) \sin \omega_2 t_0 - (\omega E_5 - m_2 E_6) \cos \omega t_0 \\ & + (\omega E_6 + m_2 E_5) \sin \omega t_0\} \end{aligned}$$

$$\begin{aligned} C_2 = & \frac{e^{-m_2 t_0}}{m_2 - m_1} \{(-\sigma y_0^* - \beta x_0^* - m_1 y_0^*) - (\omega_1 E_1 - m_1 E_2) \cos \omega_1 t_0 \\ & + (f_1 + \omega_1 E_2 + m_1 E_1) \sin \omega_1 t_0 - (\omega_2 E_3 - m_1 E_4) \cos \omega_2 t_0 \\ & + (\omega_2 E_4 + m_1 E_3 - f_2) \sin \omega_2 t_0 - (\omega E_5 - m_1 E_6) \cos \omega t_0 \\ & + (\omega E_6 + m_1 E_5) \sin \omega t_0\} \end{aligned}$$

For complex roots,

$$\begin{aligned} y^*(t) = & e^{ut}(C_1 \cos vt + C_2 \sin vt) + E_1 \sin \omega_1 t + E_2 \cos \omega_1 t + E_3 \sin \omega_2 t \\ & + E_4 \cos \omega_2 t + E_5 \sin(\omega t) + E_6 \cos(\omega t) \end{aligned} \quad (19)$$

$$x^*(t) = \left(\frac{1}{\beta}\right)(-y^* - \sigma y^* + f_1 \sin(\omega_1 t) - f_2 \sin(\omega_2 t)) \quad (20)$$

and the constants C_1 and C_2 are

$$\begin{aligned}
C_1 = & \frac{e^{-ut_0}}{v} \{((\sigma y_0^* + \beta x_0^* + u y_0^*) \sin vt_0 + v y_0^*) \cos vt_0 \\
& + ((\omega_1 E_1 - u E_2) \sin vt_0 - v E_2 \cos vt_0) \cos \omega_1 t_0 \\
& - ((f_1 + \omega_1 E_2 + u E_1) \sin vt_0 + v E_1 \cos vt_0) \sin \omega_1 t_0 \\
& + ((\omega_2 E_3 - u E_4) \sin vt_0 - v E_4 \cos vt_0) \cos \omega_2 t_0 \\
& - ((\omega_2 E_4 + u E_3 - f_2) \sin vt_0 + v E_3 \cos vt_0) \sin \omega_2 t_0 \\
& + ((\omega E_5 - u E_6) \sin vt_0 - v E_6 \cos vt_0) \cos \omega t_0 \\
& - ((\omega E_6 + u E_5) \sin vt_0 + v E_5 \cos vt_0) \sin \omega t_0\}
\end{aligned}$$

$$\begin{aligned}
C_2 = & \frac{e^{-ut_0}}{v} \{((- \sigma y_0^* - \beta x_0^* - u y_0^*) \cos vt_0 + v y_0^*) \sin vt_0 \\
& - ((\omega_1 E_1 - u E_2) \cos vt_0 + v E_2 \sin vt_0) \cos \omega_1 t_0 \\
& + ((f_1 + \omega_1 E_2 + u E_1) \cos vt_0 - v E_1 \sin vt_0) \sin \omega_1 t_0 \\
& - ((\omega_2 E_3 - u E_4) \cos vt_0 + v E_4 \sin vt_0) \cos \omega_2 t_0 \\
& + ((\omega_2 E_4 + u E_3 - f_2) \cos vt_0 - v E_3 \sin vt_0) \sin \omega_2 t_0 \\
& - ((\omega E_5 - u E_6) \cos vt_0 + v E_6 \sin vt_0) \cos \omega t_0 \\
& + ((\omega E_6 + u E_5) \cos vt_0 - v E_5 \sin vt_0) \sin \omega t_0\}
\end{aligned}$$

B. $D_{\pm 1}^*$ region

The state variables for real and distinct roots are

$$\begin{aligned}
y^*(t) = & C_3 e^{m_3 t} + C_4 e^{m_4 t} + E_7 \sin(\omega_1 t) + E_8 \cos(\omega_1 t) + E_9 \sin(\omega_2 t) \\
& + E_{10} \cos(\omega_2 t) + E_{11} \sin(\omega t) + E_{12} \cos(\omega t)
\end{aligned} \tag{21}$$

$$x^*(t) = \left(\frac{1}{\beta}\right) (-y^* - \sigma y^* + f_1 \sin(\omega_1 t) - f_2 \sin(\omega_2 t)) \tag{22}$$

and for complex roots

$$\begin{aligned}
y^*(t) = & e^{ut} (C_3 \cos vt + C_4 \sin vt) + E_7 \sin(\omega_1 t) + E_8 \cos(\omega_1 t) + E_9 \sin(\omega_2 t) \\
& + E_{10} \cos(\omega_2 t) + E_{11} \sin(\omega t) + E_{12} \cos(\omega t)
\end{aligned} \tag{23}$$

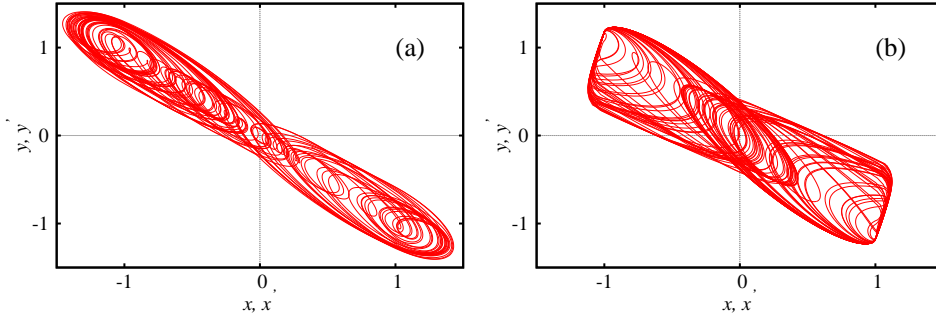


FIG. 4: Double band chaotic attractors of the transmitter and receiver systems in the $x - y$ and $x' - y'$ phase planes obtained using the analytical solutions. Chaotic attractor of the (a) *MLC* circuit and (b) the series *LCR* circuit with a *SNE*.

$$x^*(t) = \left(\frac{1}{\beta}\right)(-y^* - \sigma y^* + f_1 \sin(\omega_1 t) - f_2 \sin(\omega_2 t)) \quad (24)$$

The state variables of the difference system $x^*(t)$ and $y^*(t)$ obtained at every of instant is used to recover the information signal using Eq. 15.

The analytical solutions presented above is used to study the transmission of the information signals through chaotic masking. Two types of chaotic systems that provide the carrier signals are considered for the present study. In the first case, we consider the chaotic signal of the *Murali-Lakshmanan-Chua (MLC)* circuit and in the second case the series *LCR* circuit with a *SNE* is considered. In both the cases, the chaotic signals corresponds to the double-band chaotic attractor states. The chaotic attractors of the transmitter and receiver systems obtained from the analytical solutions given in Eqs. 9-12 in the $x - y$ and $x' - y'$ planes corresponding to the *MLC* circuit and the *SNE* circuit are shown in Fig. 4(a) and 4(b), respectively.

The *MLC* circuit is a second-order, non-autonomous chaotic circuit system having the *Chua's diode* as a nonlinear element [21] with the system parameters $a = -1.02$, $b = -0.55$, $\beta = 1$, $\nu = 0.015$, $f_{1,2} = 0.14$, $\omega_{1,2} = 0.72$. The amplitude and frequency of the sinusoidal information signal are fixed as $f = 0.5$ and $\omega = 0.25$, respectively. The recovery of the information signal obtained from the explicit analytical solutions with the *MLC* circuit

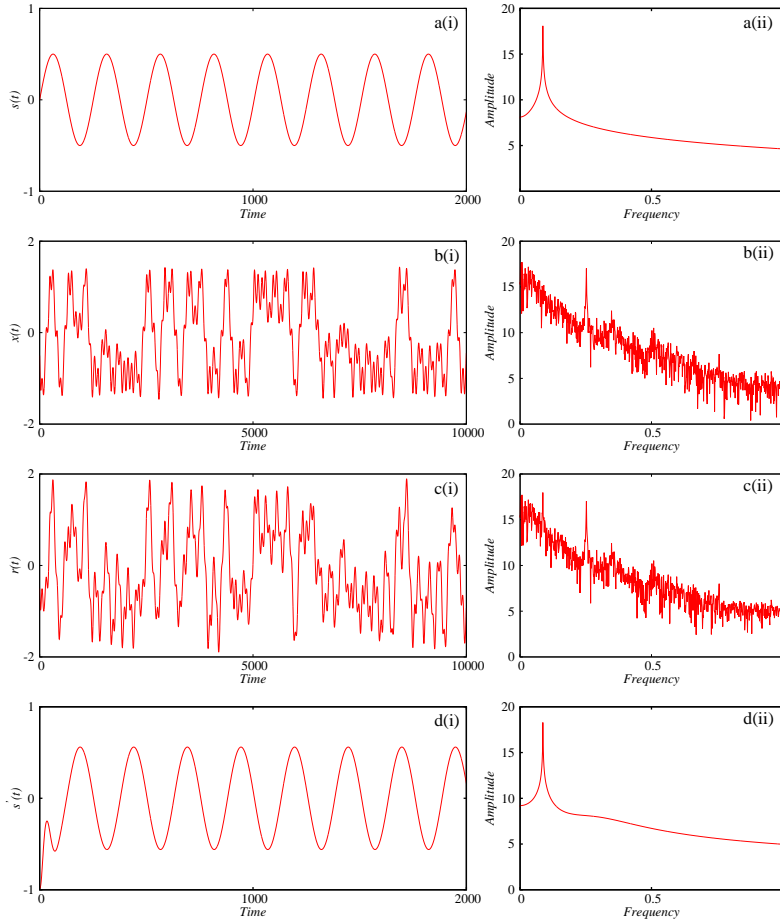


FIG. 5: *MLC* circuit. Analytical results obtained for $\epsilon = 0.85$ indicating the (i) time series and (ii) power spectrum; (a) original information signal ($s(t) = f \sin \omega t$, $F = 0.5, \nu = 0.25$ Hz); (b) chaotic carrier signal $x(t)$; (c) amplitude modulated transmitted signal $r(t) = x(t) + s(t)$ and (d) the difference signal $x^*(t)$ representing the recovered information signal $s'(t)$.

acting as the chaotic carrier is shown in Fig. 5. Figures 5a(i), b(i) and c(i) represents the analytically observed time series of the sinusoidal information signal $s(t)$, the chaotic carrier signal $x(t)$ corresponding to the transmitter system and the amplitude modulated transmitted signal, $r(t) = x(t) + s(t)$, respectively for the coupling strength $\epsilon = 0$. The power spectra corresponding to the time series given in Fig. 5a(i)-c(i) is shown in Fig. 5a(ii)-c(ii). The power spectra of the amplitude modulated chaotic transmitted wave embedding the information signal shown in Fig. 5c(ii) indicates a broad band nature resembling that of the chaotic carrier wave shown in Fig. 5b(ii) and hence the information

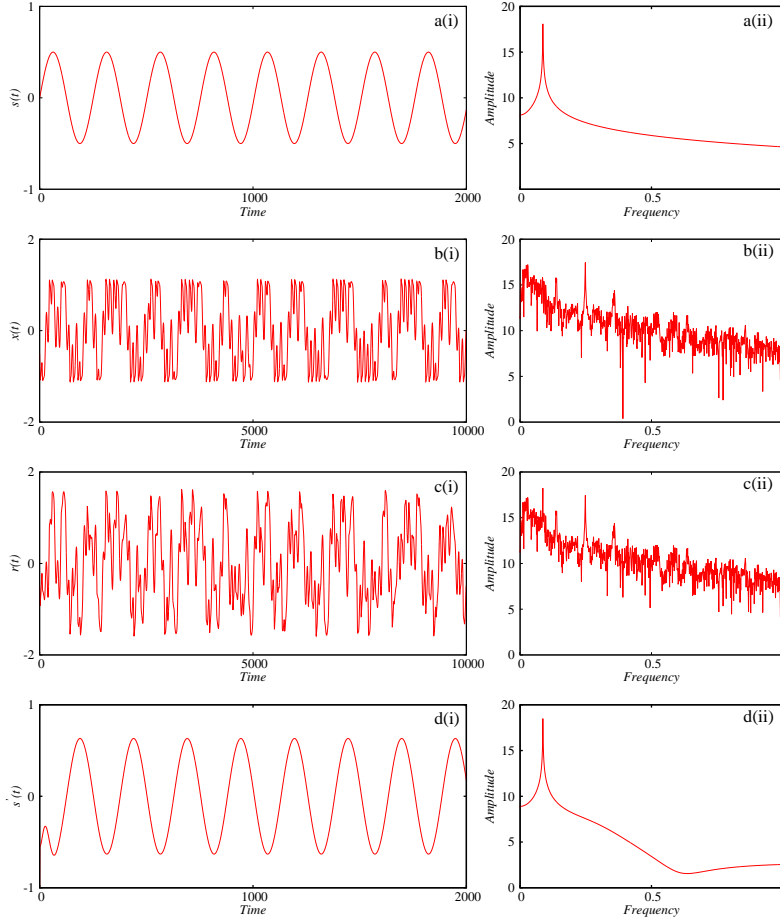


FIG. 6: Series LCR circuit with SNE . Analytical results obtained for $\epsilon = 1$ indicating the (i) time series (ii) power spectrum; (a) original information signal ($s(t) = f \sin \omega t$, $F = 0.5, \nu = 0.25$ Hz); (b) chaotic carrier signal $x(t)$; (c) amplitude modulated transmitted signal $r(t) = x(t) + s(t)$ and (d) the difference signal $x^*(t)$ representing the recovered information signal $s'(t)$.

signal is undetectable and securely masked by the chaotic carrier wave. The time series of the state variable $x^*(t)$ of the difference system representing the information signal $s'(t)$ as given by Eq. 15 and its corresponding power spectrum obtained for the coupling strength $\epsilon = 0.85$ are shown in Fig. 5d(i) and d(ii), respectively. The power spectra of the information signal $s'(t)$ recovered at the receiver shown in Fig. 5d(ii) indicates a single tone frequency nature resembling the original information signal shown in Fig. 5a(ii). Hence, the solution of the difference system $x^*(t)$ qualitatively represents the recovered signal $s'(t)$ as given in Eq. 15. The applicability of the generalized analytical solution presented above

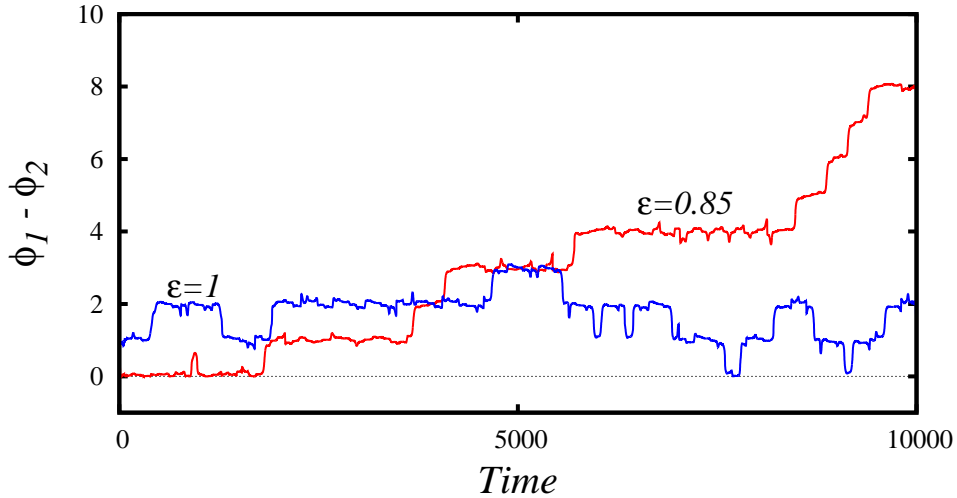


FIG. 7: Time-series of the phase difference ($\phi_1 - \phi_2$) of the transmitter and receiver systems of unidirectionally coupled *MLC* circuits (red) and *SNE* circuits (blue) indicating imperfect locking of the phases for the coupling strengths $\epsilon = 0.85$ and $\epsilon = 1$, respectively.

is studied with another circuit system namely, the series *LCR* circuit with a *simplified nonlinear element*.

The series *LCR* circuit with a *SNE* introduced by *Arulgnanam et al* [23] has the system parameter values $a = -1.148$, $b = 5.125$, $\beta = 0.9865$, $\nu = 0$, $f_{1,2} = 0.31$, $\omega_{1,2} = 0.7084$. The amplitude and frequency of the sinusoidal information signal is fixed as $f = 0.5$ and $\omega = 0.25$, respectively. The secure transmission of this information signal using the chaotic carrier signal of the *SNE* system is as shown in Fig. 6. Figures 6a(i), b(i) and c(i) represents the analytically observed time series of the sinusoidal information signal $s(t)$, the chaotic carrier signal $x(t)$ corresponding to the transmitter system and the amplitude modulated transmitted signal, $r(t) = x(t) + s(t)$, respectively for the coupling strength $\epsilon = 0$. The power spectra corresponding to the time series given in Fig. 6a(i)-c(i) is shown in Fig. 6a(ii)-c(ii). Fig. 6c(i) and c(ii) representing the time series and power spectra of the amplitude modulated chaotic transmitted wave indicates that the information signal

is undetectable and securely masked by the chaotic carrier wave. The time series of the state variable $x^*(t)$ of the difference system representing the information signal $s'(t)$ as given by Eq. 15 and its corresponding power spectrum obtained for the coupling strength $\epsilon = 1$ are shown in Fig. 6d(i) and d(ii), respectively. The power spectra of the information signal $s'(t)$ recovered at the receiver shown in Fig. 6d(ii) indicates a single tone frequency nature resembling the original information signal shown in Fig. 6a(ii). Hence, it can be confirmed that the solution of the difference system $x^*(t)$ qualitatively represents the recovered signal $s'(t)$ as given in Eq. 15. The recovered signal shown in Fig. 6d(i) indicates enhancement in the amplitude of the signal as compared to the original signal shown in 6a(i).

The nature of synchronization phenomena observed in the coupled systems can be analyzed to reveal the mechanism involved on the recovery of the information signal. From Fig. 1, it could be identified that the transmitter and the receiver systems are non-identical owing to the inclusion of the information signal at the transmitter. Recent studies on the synchronization behavior of coupled non-identical second-order, non-autonomous systems indicates the entrainment of the phases of the coupled systems with the increase in coupling strength [27]. Figure 7 indicates the imperfect locking of the phases of the coupled MLC (red) and *simplified nonlinear element* (blue) circuit systems for the coupling strengths $\epsilon = 0.85$ and $\epsilon = 1$, respectively. Hence, the signals corresponding to the state variables of the coupled systems undergo imperfect locking of phases and the transmitted and recovered information signals always have a phase difference as shown in Fig. 7. From the above discussions, it is observed that the solution of the difference system ($x^*(t)$) is a qualitative measure of the information signal ($s'(t)$) recovered at the receiver system as given by Eq. 15. This behavior has been confirmed in two types of chaotic systems discussed above and the nature of the synchronization phenomena observed in the coupled systems during the signal recovery is identified.

IV. NUMERICAL RESULTS

In this section, we present the numerical simulation results for signal transmission achieved through synchronization of chaotic systems. The normalized state equations of the coupled transmitter and receiver system given in Eqs. 5 and 6 are simulated for two

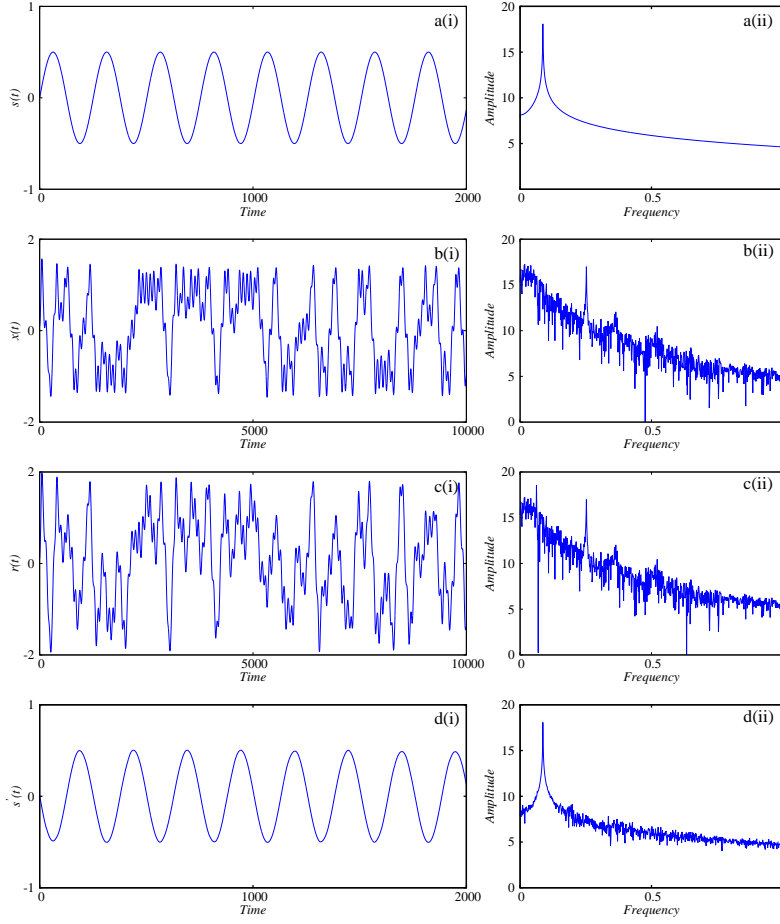


FIG. 8: *MLC* circuit. Numerical results obtained for $\epsilon = 12$ indicating the (i) time series and (ii) power spectrum; (a) original information signal ($s(t) = f \sin \omega t$, $F = 0.5, \nu = 0.25$ Hz); (b) chaotic carrier signal $x(t)$; (c) amplitude modulated transmitted signal $r(t) = x(t) + s(t)$ and (d) the recovered information signal $s'(t)$.

different system parameters corresponding to the the *MLC* and *SNE* circuits to validate the analytical results. Figure 8 shows the numerical results obtained for the system parameters $a = -1.02$, $b = -0.55$, $\beta = 1$, $\nu = 0.015$, $f_{1,2} = 0.14$, $\omega_{1,2} = 0.72$ corresponding to the *MLC* circuit system. Figures 8a(i), b(i) and c(i) represents the numerically observed time series of the sinusoidal information signal $s(t)$, the chaotic carrier signal $x(t)$ and the amplitude modulated transmitted signal, $r(t) = x(t) + s(t)$, respectively for the coupling strength $\epsilon = 0$. The power spectra corresponding to the time series of the signals given in Fig. 8a(i)-c(i) are shown in Fig. 8a(ii)-c(ii). The undetectable nature of the information signal

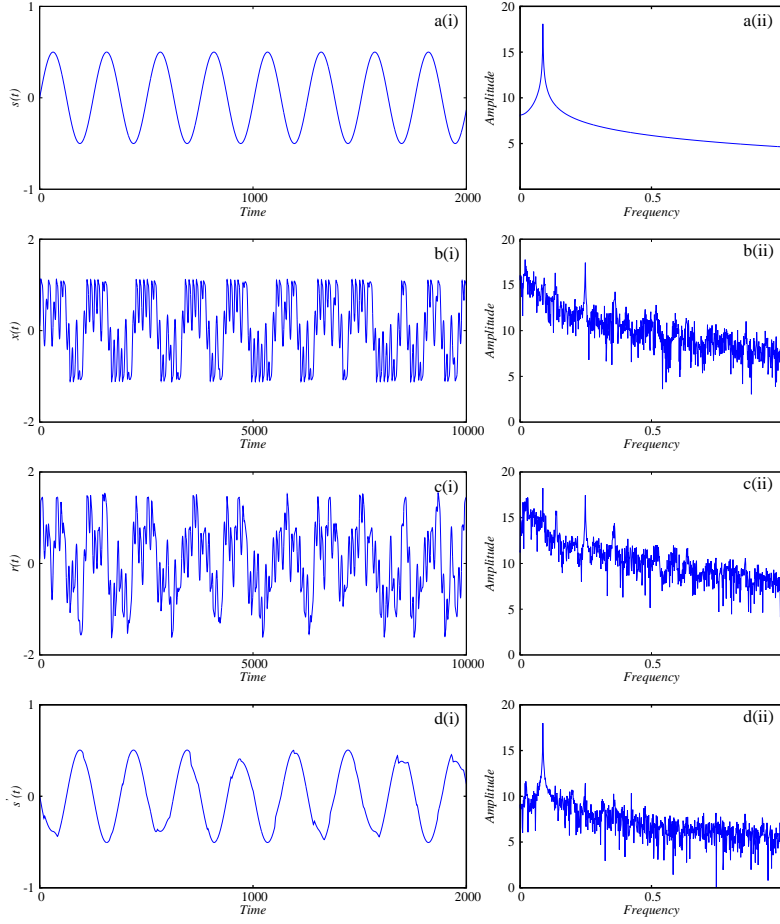


FIG. 9: Series LCR circuit with SNE . Numerical results obtained for $\epsilon = 20$ indicating the (i) time series (ii) power spectrum; (a) original information signal ($s(t) = f \sin \omega t$, $F = 0.5$, $\nu = 0.25$ Hz); (b) chaotic carrier signal $x(t)$; (c) amplitude modulated transmitted signal $r(t) = x(t) + s(t)$ and (d) the recovered information signal $s'(t)$.

owing to chaotic masking is represented by the amplitude modulated transmitted wave and its corresponding power spectrum shown in Fig. 8c(i) and c(ii), respectively. The time series of the recovered information signal $s'(t)$ and its corresponding power spectrum obtained for the coupling strength $\epsilon = 12$ are shown in Fig. 8d(i) and d(ii), respectively. The power spectra of the information signal $s'(t)$ recovered at the receiver shown in Fig. 8d(ii) indicates a single tone frequency nature resembling the original information signal shown in Fig. 8a(ii). It has to be noted that the recovered information signal $s'(t)$ presented in Fig. 8d(i) is actually the difference signal $x(t) - x'(t)$ i.e. $s'(t) = x(t) - x'(t)$.

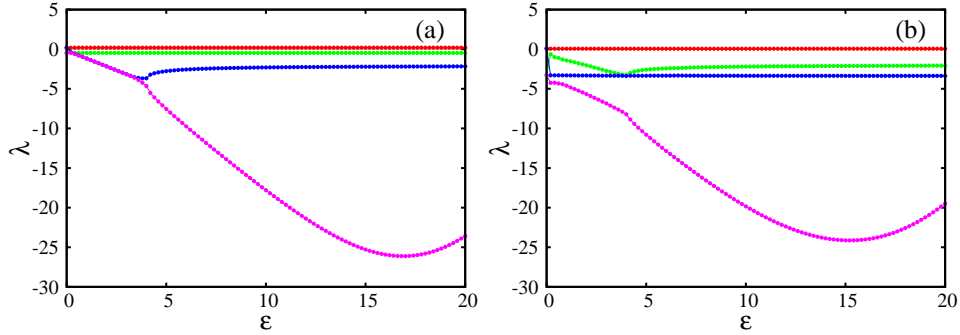


FIG. 10: The four largest Lyapunov exponents of the unidirectionally coupled chaotic systems corresponding to (a) *MLC* circuits and (b) series *LCR* circuits with *SNE*.

The numerical results showing the recovery of information signal observed in coupled series *LCR* circuits with *SNE* for the system parameters $a = -1.148$, $b = 5.125$, $\beta = 0.9865$, $\nu = 0$, $f_{1,2} = 0.31$, $\omega_{1,2} = 0.7084$ is shown in Fig. 9. Figures 9a(i), b(i) and c(i) represents the numerically observed time series of the sinusoidal information signal $s(t)$, the chaotic carrier signal $x(t)$ and the amplitude modulated transmitted signal, $r(t) = x(t) + s(t)$, respectively for the coupling strength $\epsilon = 0$. The power spectra corresponding to the time series of the signals given in Fig. 9a(i)-c(i) are shown in Fig. 9a(ii)-c(ii). The undetectable nature of the information signal owing to chaotic masking is represented by the amplitude modulated transmitted wave and its corresponding power spectrum shown in Fig. 9c(i) and c(ii), respectively. The time series of the recovered information signal $s'(t)$ and its corresponding power spectrum obtained for the coupling strength $\epsilon = 20$ are shown in Fig. 9d(i) and d(ii), respectively. The power spectra of the information signal $s'(t)$ recovered at the receiver shown in Fig. 9d(ii) indicates a single tone frequency nature resembling the original information signal shown in Fig. 9a(ii). The broadband nature of the recovered signal observed in the power spectra shown in Fig. 8d(ii) and 9d(ii) are due to numerical artifacts. The largest Lyapunov exponents of the coupled system given by Eqs. 5 and 6 indicating the synchronized nature for the two types of system parameters are presented in Fig. 10.

V. CONCLUSION

We have reported in this paper, an explicit generalized analytical solution for a simple communication scheme involved in the transmission and recovery of an information signal. The waveform of two simple chaotic systems have been used as the carrier to mask the information signal. The analytical results leads to the following important conclusions. The state variable of the difference system indicates a measure of the information signal recovered at the receiver. The transmitter and the receiver systems does not synchronize completely and undergo imperfect locking of their phases at higher values of coupling strength. The amplitude of the recovered signal has been enhanced during its retrieval at the receiver. The numerical results presented validates the claim that the recovered signal is obtained from the difference of the coupled state variables. The analytical and numerical results are confirmed through electronic circuit experimental results. The transmission and recovery of information signal using a simple communication scheme studied through explicit analytical solutions is reported in the literature for the first time.

-
- [1] M. Pecora and T. L. Carroll, *Physical Review Letters* **64**, 821 (1990).
 - [2] N. F. Rulkov, A. R. Volkoskii, A. Rodríguez-Lozano, E. Del Río, and M. G. Velarde, *International Journal of Bifurcation and Chaos* **02**, 669 (1992), <https://doi.org/10.1142/S0218127492000781>, URL <https://doi.org/10.1142/S0218127492000781>.
 - [3] L. O. Chua, L. Kocarev, K. Eckert, and M. Itoh, *International Journal of Bifurcation and Chaos* **02**, 705 (1992), <https://doi.org/10.1142/S0218127492000811>, URL <https://doi.org/10.1142/S0218127492000811>.
 - [4] L. O. Chua, M. Itoh, L. Kocarev, and K. Eckert, *Journal of Circuits, Systems and Computers* **03**, 93 (1993), <https://doi.org/10.1142/S0218126693000071>, URL <https://doi.org/10.1142/S0218126693000071>.
 - [5] K. Murali and M. Lakshmanan, *Phys. Rev. E* **48**, R1624 (1993), URL <https://link.aps.org/doi/10.1103/PhysRevE.48.R1624>.
 - [6] S. Boccaletti, J. Kurths, G. Osipov, D.L. Valladares, and C.S. Zhou, *Physics Reports* **366**, 1

- (2002).
- [7] A. V. Oppenheim, G. W. Wornell, S. H. Isabelle, and K. M. Cuomo, in *[Proceedings] ICASSP-92: 1992 IEEE International Conference on Acoustics, Speech, and Signal Processing (1992)*, vol. 4, pp. 117–120, ISSN 1520-6149.
 - [8] K. Murali and M. Lakshmanan, *Phys. Rev. E* **49**, 4882 (1994), URL <https://link.aps.org/doi/10.1103/PhysRevE.49.4882>.
 - [9] K. Murali and M. Lakshmanan, *Phys. Rev. E* **56**, 251 (1997), URL <https://link.aps.org/doi/10.1103/PhysRevE.56.251>.
 - [10] A. A. Koronovskii, O. I. Moskalenko, and A. E. Hramov, *Physics-Uspekhi* **52**, 1213 (2009), ISSN 1468-4780, URL <https://doi.org/10.3367%2Fufne.0179.200912c.1281>.
 - [11] K. Murali, , V. Varadan, and H. Leung, *IEEE Transactions on Consumer Electronics* **47**, 709 (2001), ISSN 0098-3063.
 - [12] K. Murali, H. Leung, K. Shakthi Preethi, and I. Raja Mohamed, *IEEE Transactions on Consumer Electronics* **49**, 59 (2003), ISSN 0098-3063.
 - [13] Z. Wu, X. Zhang, and X. Zhong, *IEEE Access* **7**, 37989 (2019), ISSN 2169-3536.
 - [14] J. Wang, W. Yu, J. Wang, Y. Zhao, J. Zhang, and D. Jiang, *International Journal of Circuit Theory and Applications* **47**, 702 (????), <https://onlinelibrary.wiley.com/doi/pdf/10.1002/cta.2617>, URL <https://onlinelibrary.wiley.com/doi/abs/10.1002/cta.2617>.
 - [15] U. E. Kocamaz, S. Çiçek, and Y. Uyaroğlu, *Journal of Circuits, Systems and Computers* **27**, 1850057 (2018).
 - [16] M. Borah and B. Roy (2018), pp. 1–6.
 - [17] S. Çiçek, U. E. Kocamaz, and Y. Uyaroğlu, *AEU - International Journal of Electronics and Communications* **88**, 52 (2018), ISSN 1434-8411, URL <http://www.sciencedirect.com/science/article/pii/S1434841117322847>.
 - [18] H. P. Ren, C. Bai, Z.-Z. Huang, and C. Grebogi, *International Journal of Bifurcation and Chaos* **27**, 1750076 (2017), <https://doi.org/10.1142/S0218127417500766>, URL <https://doi.org/10.1142/S0218127417500766>.
 - [19] Y. Liu, L. Li, and Y. Feng, *ASME. J. Comput. Nonlinear Dynam.* **11**, 051028 (2016).
 - [20] S. Saini and J. S. Saini, in *2014 International Conference on Parallel, Distributed and Grid Computing (2014)*, pp. 159–163.

- [21] K.Murali, M.Lakshmanan, and L. O. Chua, IEEE Transactions on Circuits and Systems-I: Fundamental Theory and Applications **41**, 462 (1994).
- [22] K. Thamilmaran, M. Lakshmanan, and K. Murali, International Journal of Bifurcation and Chaos **10(7)**, 1175 (2000).
- [23] A. Arulgnanam, K. Thamilmaran, and M. Daniel, Chaos, Solitons and Fractals **42**, 2246 (2009).
- [24] A. Arulgnanam, K. Thamilmaran, and M. Daniel, Chinese Journal of Physics **53**, 060702 (2014).
- [25] G.Sivaganesh, Chinese Physics Letters **32**, 010503 (2015).
- [26] G. Sivaganesh and A. Arulgnanam, Chinese Physics B **26**, 050502 (2017).
- [27] G. Sivaganesh, A. Arulgnanam, A. N. Seethalakshmi, and S. Selvaraj, Journal of the Korean Physical Society **72**, 1121 (2018), ISSN 1976-8524, URL <https://doi.org/10.3938/jkps.72.1121>.
- [28] G. Sivaganesh, A. Arulgnanam, and A. Seethalakshmi, Chaos, Solitons & Fractals **113**, 294 (2018), ISSN 0960-0779, URL <http://www.sciencedirect.com/science/article/pii/S096007791830359X>.
- [29] B. Jovic, S. Berber, and C. Unsworth, Physica D: Nonlinear Phenomena **213**, 31 (2006), ISSN 0167-2789, URL <http://www.sciencedirect.com/science/article/pii/S0167278905004598>.
- [30] *Chaos in Nonlinear Oscillators: Controlling and Synchronization* (World Scientific Series on Nonlinear Science, Singapore, 1996).